ISTITUTO NAZIONALE DI GEOFISICA E VULCANOLOGIA

Velocity profile report at the seismic station IV.TERO – TERAMO (TE)

Report sul profilo di velocità sismica per il sito della stazione sismica IV.TERO – TERAMO (TE)

Working Group: **Giuseppe Di Giulio** **Maurizio Vassallo** **Giovanna Cultrera** **Luca Minarelli**	Date: Dicembre 2019
Subject: **Final report illustrating measurements, analysis and results for Vs profile at station IV.TERO**	

INDEX

1. Introduction 4

2. Geophysical Investigations 5

2.1 Single-station noise measurements 8
2.2 2D passive array of vertical geophones 13
2.3 1D active array of vertical geophones 14

3. Seismic Velocity Model 18

4. Conclusions 21

References 22
Disclaimer and limits of use of information 23
Esclusione di responsabilità e limiti di uso delle informazioni 24

1. INTRODUCTION

In this report, we present the geophysical measurements and the results obtained in the framework of the agreement between INGV and DPC 2019-2021, All. B2-WP1, Task2 (Coordinator: G. Cultrera, F. Pacor)" for the site characterization of stations belonging to the national seismic networks (IV and IT).

Here the results of the IV.TERO station (Teramo, Central Italy) are presented.

Please note that IV.TERO is on Teramo municipality, but this station is situated at the top of a mountain relief at about 8 km from the city of Teramo, near the hamlet named Valle San Giovanni (TE). A seismic strong-motion station is also present within the city with name IT.TER, which belongs to IT seismic network.

Geophysical measurements in proximity of IV.TERO were carried out between July and September 2019. They are composed of several single-station ambient vibrations (or seismic noise) measurements, a two 2D arrays with circular geometry of vertical geophones in passive configuration, and a 1D array with linear geometry of vertical geophones using a 5 Kg hammer as active source.

Based on horizontal-to-vertical (HV) spectral ratios and surface-wave analysis, we provide results in terms of HV curves and surface-wave dispersion curves. Dispersion curves are inverted to obtain the shear-wave velocity (Vs) profile for the studied area. The Vs models are used for computing the average velocity in the uppermost 30 m (V_{s30}) and assigning then the EC8 or NTC soil class category.

2. GEOPHYSICAL INVESTIGATIONS

Fig. 1 shows the location of the IV.TERO station (latitude 42.62279; longitude 13.60393 as reported in https://www.fdsn.org/networks/detail/IV/). We note that such position falls in proximity of the fence where antenna and digitizer of the station are, although the sensors of IVI.TERO (velocimeter and accelerometer) are placed in an inspection pit distant about 15 m SE from the yellow marker of Fig. 1 (see also Fig. 4). The pit cover is visible in grey after a zoom of Fig. 1

Figure 1: Google map with the position of IV.TERO site (yellow marker).

Starting from the available information reported in the monograph of ESM-Engineering Strong-Motion database (Luzi et al. 2016), IV.TERO shows HV noise spectral ratios almost flat (Fig. 2), with a weak peak at about 1.3 Hz. HV curve computed on earthquakes is consistent, with a weak peak identified even at high frequency (11.8 Hz).

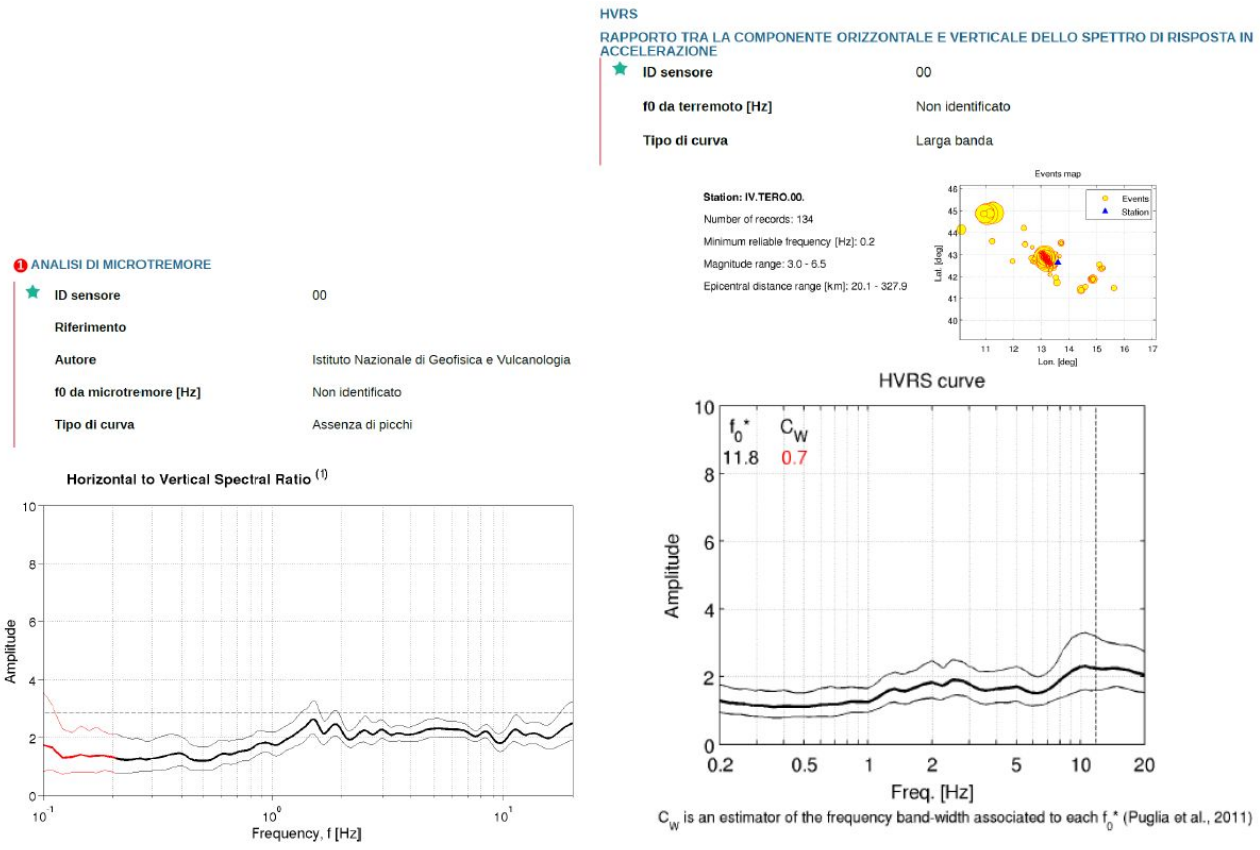

Figure 2: Redrawn from the site monograph reported in ESM database (Luzi et al. 2016). On the left HV noise spectral ratio, on the right HV ratios computed on earthquakes.

Fig. 3 shows the new geophysical measurements analyzed in the present report using the *GEOPSY* tool (www.geopsy.org). In proximity of IV.TERO, we performed simultaneously several noise measurements with stations arranged on the slope approximately in a cross geometry (see Fig. 3). These stations were deployed for about 3 hours on the 25th of July 2019, a sunny day characterized by high temperature and absence of wind. 6 stations (TB00, TB01, TB02, TB03, TB04 and TB05) were deployed following the main slope of the relief; other three stations (TB06, REFTE07 and REFTE08) were deployed orthogonal to the main slope. TB indicates TERRABOT instruments (wifi equipment manufactured by SARA electronics) composed of 4.5 Hz geophones along the three directions of motion (yellow markers in the right portion of Fig. 3), whereas REF indicates REFTEK digitizers coupled to the Le3d-5s velocimeter (red markers in Fig. 3). Some other 4 single-stations measurements were repeated the 31th of July 2019 (sunny day with absence of wind) just at the top and at the bottom of the inspection pit (see following paragraph).

Due to the slope of the site, we prefer to arrange (25th of July) a 2D passive array of vertical 4.5 Hz geophones (in number of 24) in a more flat field to the western, at a distance of about 100 m with respect to the IV.TERO position (Fig. 3). The 2D array of 24 vertical geophones was deployed in a circular geometry along two rings. The radius of the inner and outer ring was around 13 m and 25 m, respectively. A noise measurements was also recorded in the field of the 2D array using a Reftek and Le3d5s equipment (red marker named REFT03 in Fig. 3). Because the result (in terms of dispersion curve) of the 2D passive array of 24 geophones was not satisfactory, we finally carried out (6 September 2019; sunny day and no wind) a linear array of 4.5 Hz vertical geophones in the same field (see the black line in Fig. 3) using a 5Kg hammer as active source. A single-station measurements was further performed during the linear array in proximity of the last geophone (the noise measurements is indicated as CH72 in Fig. 3). We used the results of the linear array to derive a dispersion curve.

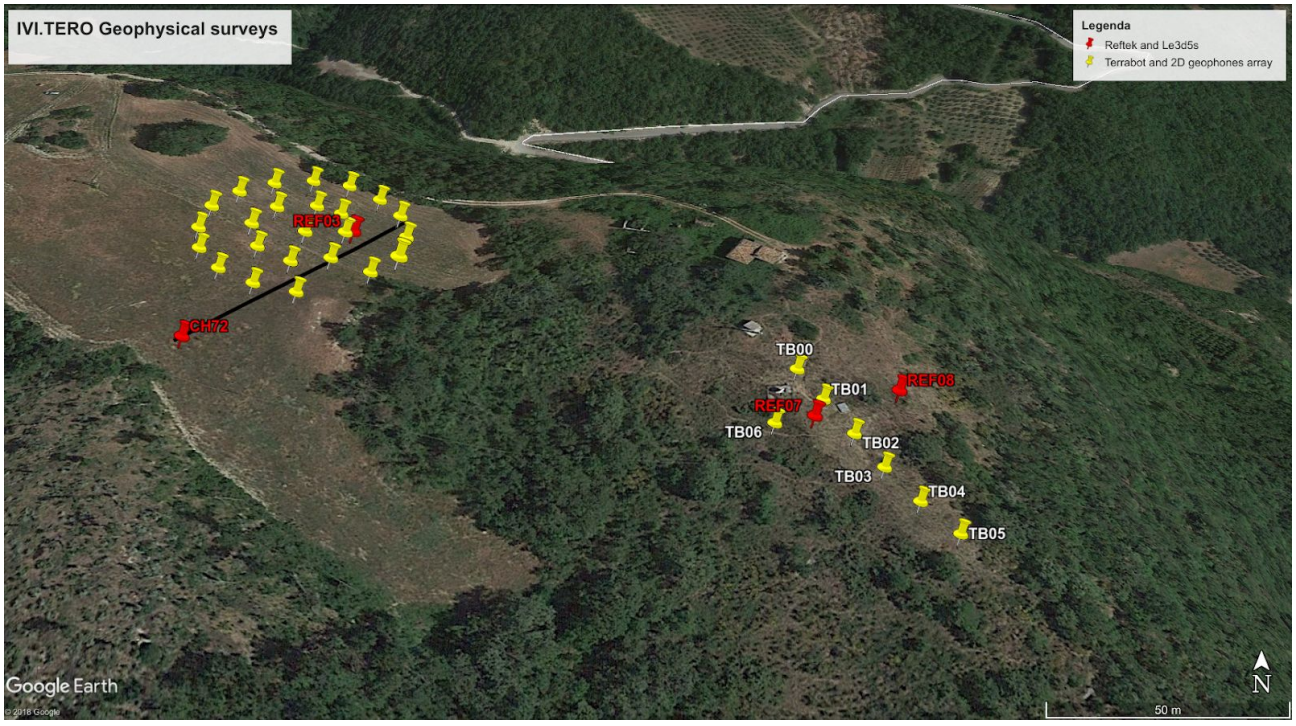

Figure 3: Geophysical surveys performed between July and September 2019. On the right part of the figure, it is reported the single-station measurements points deployed around the IV.TERO station with almost a cross geometry (yellow and red markers indicates Terrabot and Reftek connected to Le3d5s, respectively). On the left part of the map, it is visible the 2D passive array (4.5 Hz vertical geophones in number of 24, yellow markers) and the single-station noise measurement (performed on the same day of the 2D array; red marker). The linear active array of 4.5 Hz vertical geophones (in number of 72, equally spaced of 1m) is shown as black line, and the red symbol indicates the single-station noise measurements (named CH72) in proximity of the last geophone.

2.1 Single-Station Noise measurements

Fig. 4 shows the field area around IV.TERO. The two pictures are taken from the top and the bottom along the main slope direction. TB00, TB01, TB02, TB03, TB04 and TB05 were deployed at a distance of 10 m each other on the red line along the maximum slope (Fig. 3), TB06 REF07 and REF08 in an orthogonal direction. A variability of the HV noise spectral ratios (Fig. 5) is visible among the stations. Both REF07 and REF08 sites (Reftek130 connected to Le3d-5s) show a low-frequency peak around 0.4 Hz. TB00 and TB01 also show HV curves with a bump in the low frequency range. The remaining sites of Fig. 5 are characterized by an almost flat HV curve (in accord with the information into ESM database; Fig. 2).

Fig. 6 shows a comparison for all the measurements performed with the most suitable equipment in the lower frequency band (Reftek130 with Le3d-5s). The three simultaneous measurements REF03 REF07 and RF08 (operating the 25th of July 2019) show the low-frequency peak at 0.4 Hz (with directional effects especially evident at REF08); one measurement (CH72 collected the 6th of September 2019) does not show the low-frequency peak.

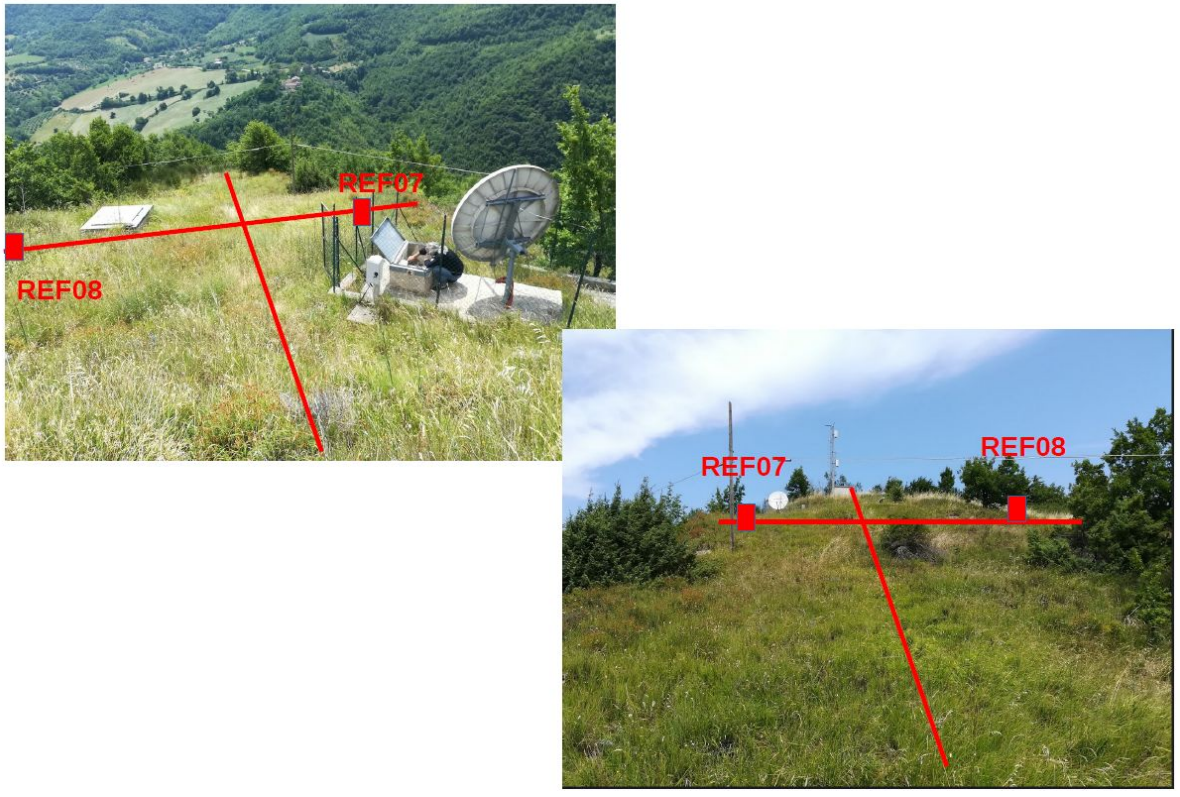

Figure 4: Pictures showing IV.TERO area. The antenna and digitizer are located within the fenced area (where the operator is). The sensors of IV.TERO are set into the inspection pit outside the fence. The two red lines show the alignments where we deployed the Terrabot and the Reftek+Le3d5s stations (only the position of REF07 and REF08 are reported for simplicity).

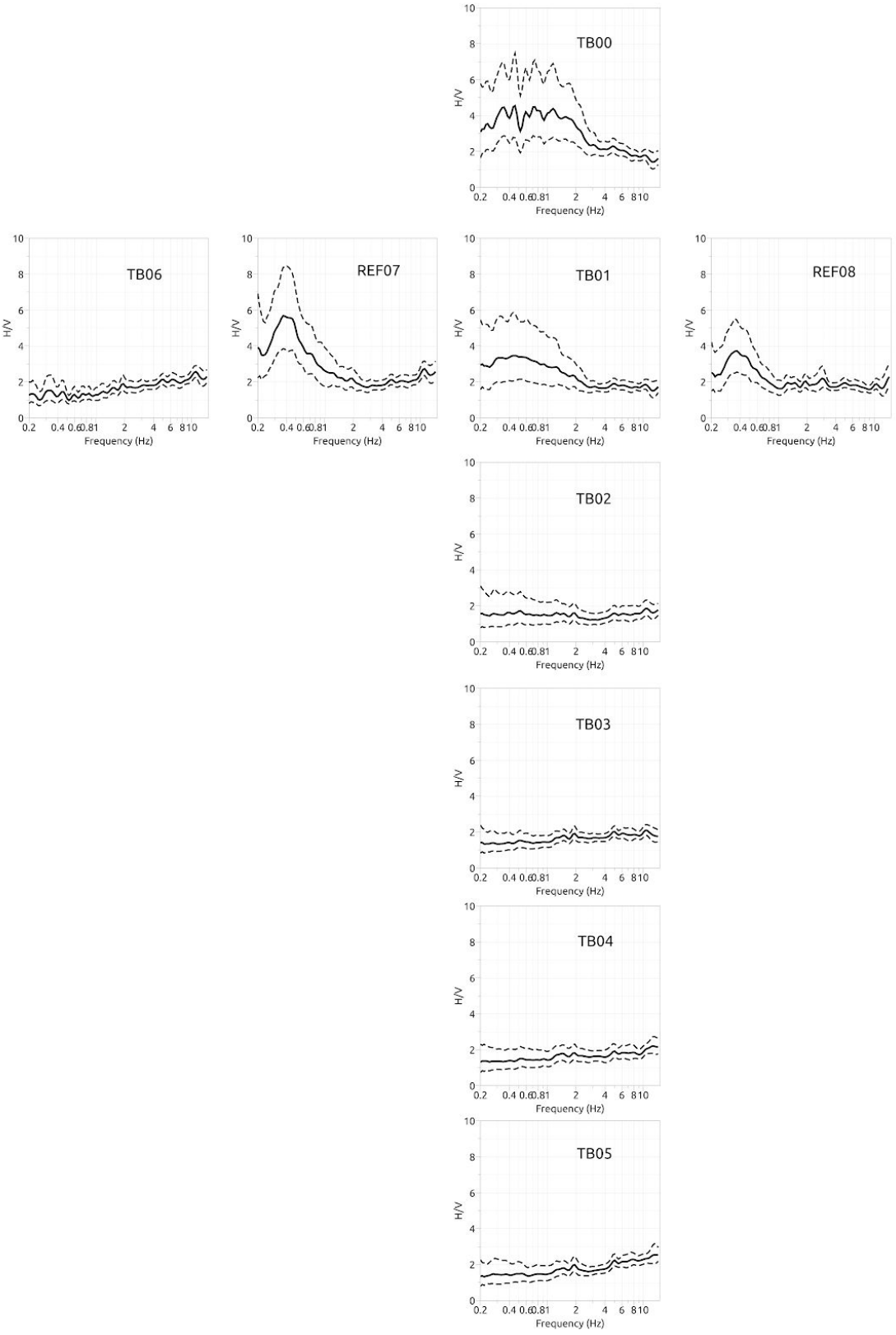

Figure 5: HV noise spectral ratios for sites TB00, TB01, TB02, TB03, TB04, TB05 (along the maximum slope) and TB06, REF07 and REF08 (orthogonally to the maximum slope).

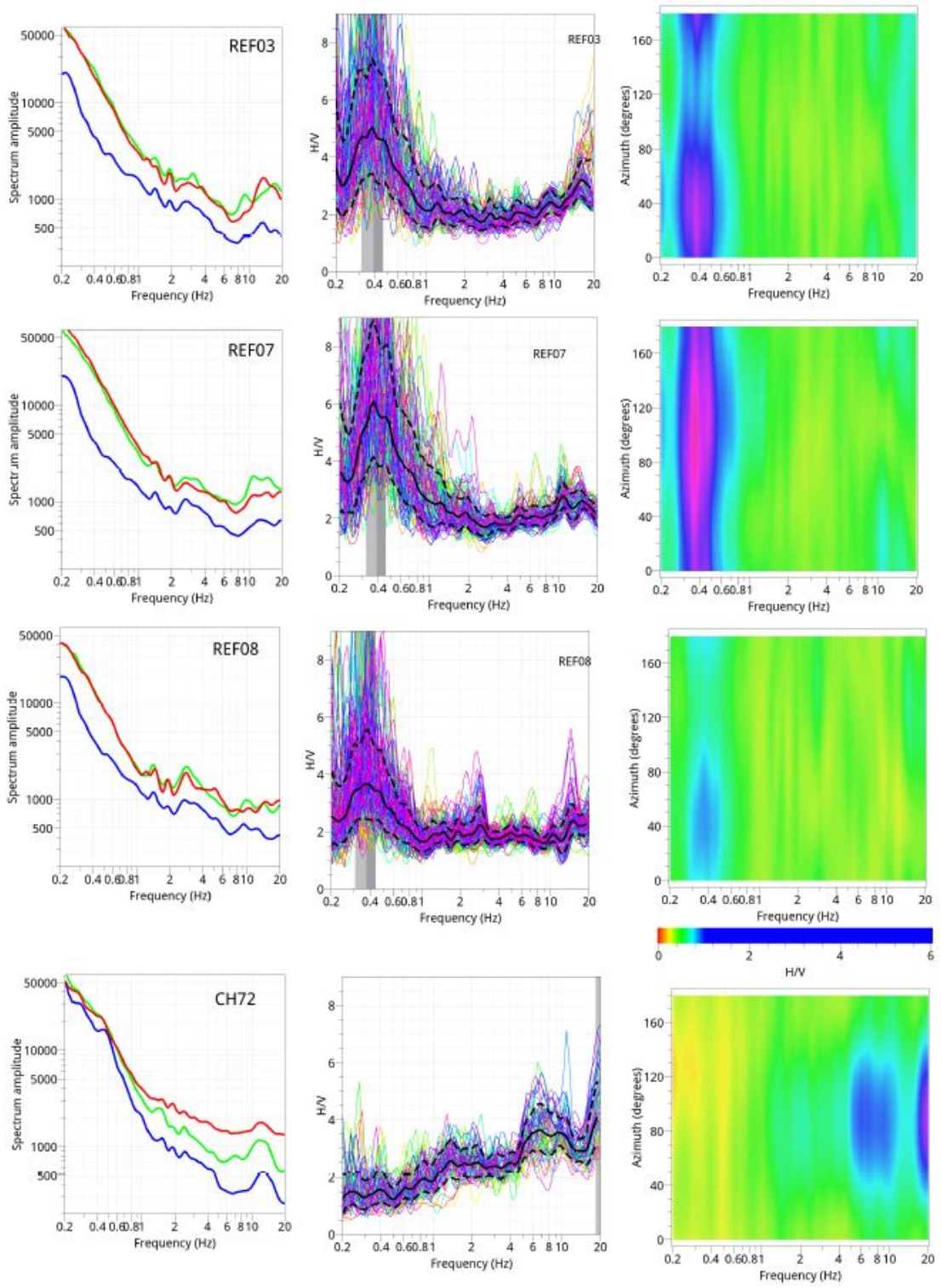

Figure 6: Fourier Amplitude Spectra of the three components of motion (blue curve refers to the vertical component), HV noise spectral ratios and rotating HV ratios for sites REF03, REF07, REF08 and CH72. All stations have a similar equipment (Reftek130 with Le3d5s). Measurements REF03 REF07 and REF08 were carried out on the 25th of July 2019, measurement CH72 on the 6th of September 2019 (see Fig. 3 for their position).

To better investigate the reliability of the low-frequency peak observed at 0.4 Hz, other single-station measurements were repeated the 31th of July 2019. We set a couple of Reftek130 connected to Le3d5s with a Terrabot both at the surface and into the inspection pit, respectively (Fig. 7). The couple of stations at the surface and at the bottom of the pit recorded simultaneously for about 2 hours (Fig. 8), and the resulting HV ratios show the presence of the low-frequency peak only for station at the surface, especially evident for the Reftek connected to the Le3d5s. Interestingly, the HV curves are almost flat at the bottom of the pit (about 2 m deep), consistently with the shape reported in ESM databases.

During our surveys IV.TERO was not working properly, and for this reason we cannot consider its recording simultaneous to our experiments. In any case, CRISP database already reported the HV noise analysis performed on IV.TERO considering 24 hours of 12th April 2015. The results (Fig. 9) show still HV curves without strong peak (mean amplitude below 2) and with some directional effects (magnification almost on the NS component).

To conclude on HV curves, we do not have an interpretation of the low-frequency (about 0.4 Hz) peak occurred at the surface at the measurements in July 2009, but we believe it as unreliable. In our opinion, the HV curves almost flat available in ESM or CRISP database are reliable.

Figure 7: A Reftek130 connected to Le3d5s together with a Terrabot were situated at the surface (on the left) and at the bottom (on the right) of the inspection pit. Measurements were carried out on the 31th of July 2019.

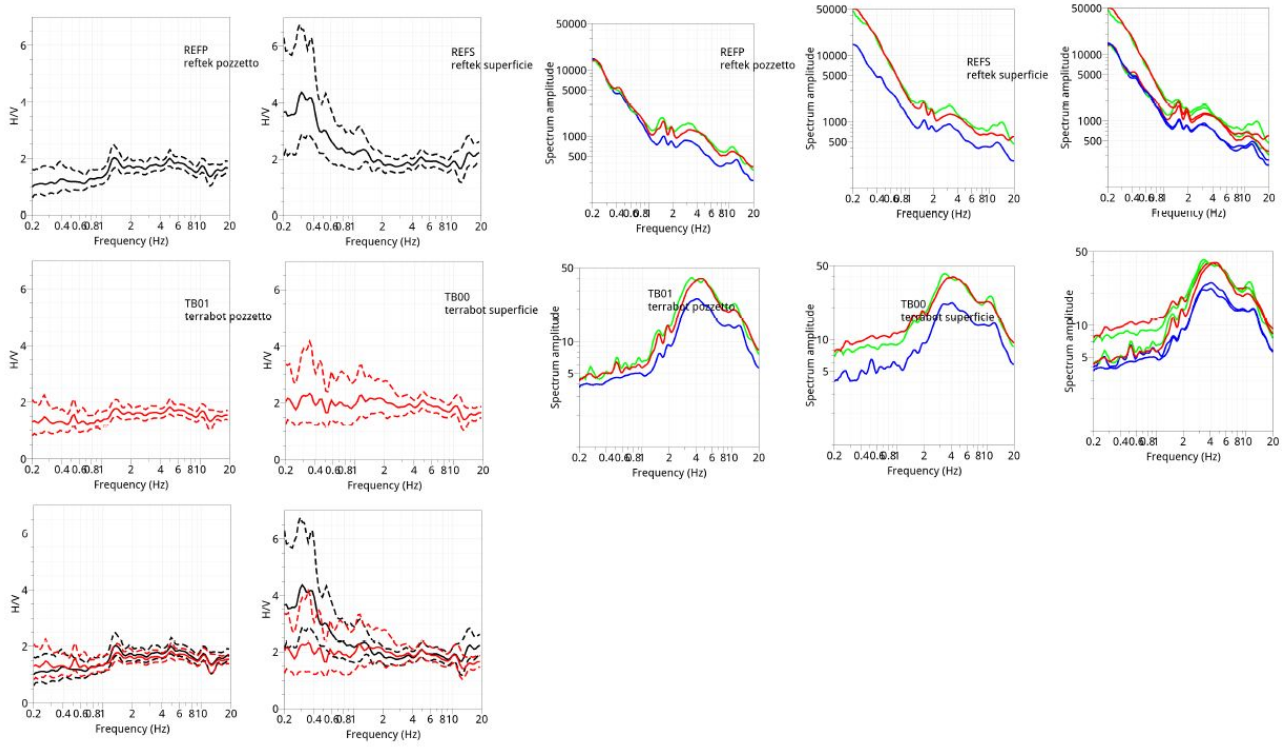

Figure 8: HV curves resulting at the surface and at the bottom of the pit (see Fig. 7). The first column shows the HV results of the bottom couple (black curves refer to Reftek + Le3d5s; red curve refer to Terrabot) and their comparison. The second column shows the HV curves at the surface (black curves refer to Reftek + Le3d5s; red curve refer to Terrabot). The other columns show the Fourier Amplitude spectra (arbitrary units) of the three-components of motion for the bottom couple (third column), of the top couple (fourth column) and their comparison (sixth column).

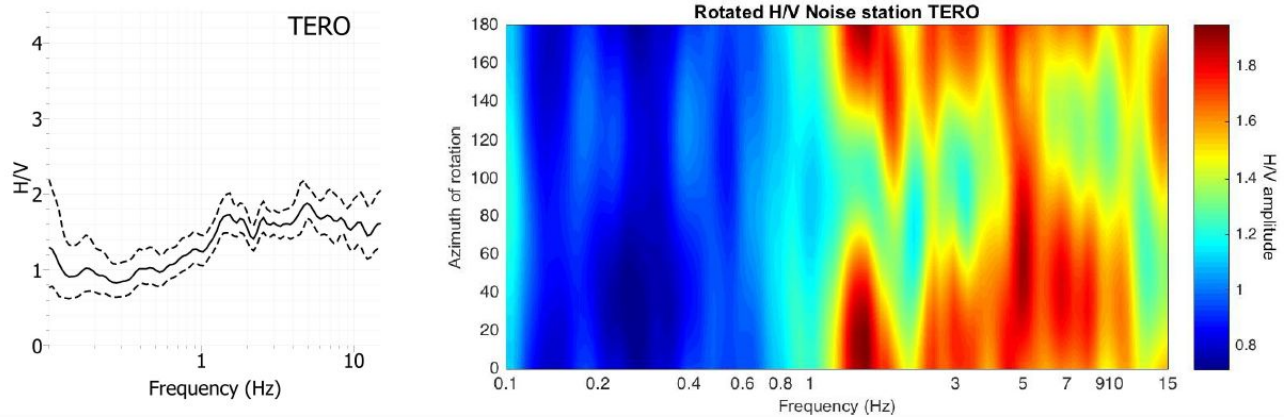

Figure 9: HV ratios and rotating HV curves as reported from crisp database (http://crisp.int.ingv.it) computed on 24 hours of 12th April 2015.

2.2 2D passive array of vertical geophones

2D passive array was performed using 24 vertical geophones (*GS11D* manufactured by *Geospace*, sensitivity 28V/m/s) with eigen-frequency of 4.5 Hz. Due to the logistic difficulty linked to the slope in proximity of IV.TERO, the 2D array was deployed in a field at about 100 m far from the seismic station (a map view of the field work is in Fig. 3), where no significant geological variations are expected (see the Geological Report http://hdl.handle.net/2122/12959). A picture of the grass field and a zoomed view of the array geometry is reported in Fig. 10. The 24 geophones were connected to two *Geode* multistations (manufactured by *Geometrics*), and we have recorded noise signal for a total duration of 64 minutes (16 records each 4 minutes length) with a sampling of 0.004 sec (250 Hz). The only possible disturb in the array field was the power line (visible in Fig. 10 left panel), with a 50 Hz that was recognized in the recordings during the check step especially for the geophones closest to the electric line.

Figure 10: On the left a picture of the field where the 2D passive array was set, on the right a map with the geometry. The yellow markers indicate the 24 vertical geophones (eigenfrequency 4.5 Hz). The red markers show single-station noise measurement (REF03 and CH72 discussed before). The black line indicates the position of the linear active array (71 m long) performed about 2 weeks later (6th of September 2019).

Data from the 2D arrays of geophones have been analysed in terms of conventional frequency-wavenumber (f-k) analysis on the vertical signal using the tool developed in *GEOPSY* (http://www.geopsy.org). Fig. 11 shows the results. In this case the f-k analysis does not provide satisfactory results, with a surface-wave dispersion curve that cannot be recognized. Fig. 11 shows a doubitatively velocity at about 350 m/s at very high-frequency. After several tests within *GEOPSY* (using different parameters in the processing step and different limits in the *max2curve* command), we conclude that the values of surface wave-velocities at 1200-1400 from Fig. 11 are not reliable.

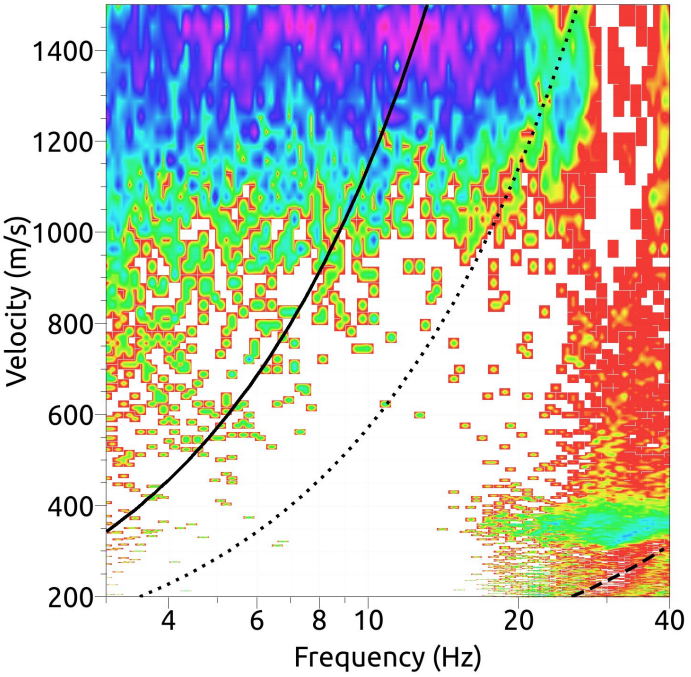

Figure 11: f-k result from the 2D passive array using 24 vertical geophones (eigenfrequency 4.5 Hz). A surface-wave dispersion curve cannot be detected. Theoretical resolution (Kmin/2, Kmin) and alias limits (Kmax/2) are also overlaid as black curves.

2.3 1D active array of vertical geophones

Because the results obtained from 2D passive array were not satisfactory, we repeated some days later (the 6th of September 2009) a linear array of geophones in the same field of the 2D array (black line in Fig. 10). We used 72 vertical geophones (same typology of the ones used in the 2D array) equally spaced of 1 m and 3 multi-channels *Geode* systems. As active source we used a sledge-hammer of 5kg, with the offset of the shots set equal to -5m and -1m from the first geophone, equal to 35.5 m (in the middle of the layout), and equal to +1m and +5m from the last geophone (#72). For each offset, we repeated the shots 3 times to increase the signal-to-noise ratios. We recorded each signal with a sampling of 0.000125 sec (8000 Hz) for a duration of 2 sec.

Fig. 12 shows an example of a recorded signal (reverse shot) in time domain. The f-k results for each shot are shown in Fig. 13. The f-k spectra for the same offset were stacked (last column in Fig. 13), and a dispersion curve was picked (black lines with error bars in Fig. 13). The resulting surface-wave dispersion curves are fairly consistent at all files; the values of apparent velocities are ranging from approximately 200-250 m/s at 80 Hz to 500-600 m/s at about 30 Hz. Because the most

continuous dispersion curves were obtained with offset -5 and -1 m, we used these ones in the inversion step.

The comparison in terms of f-k curves between active and passive array is shown in Fig. 14.

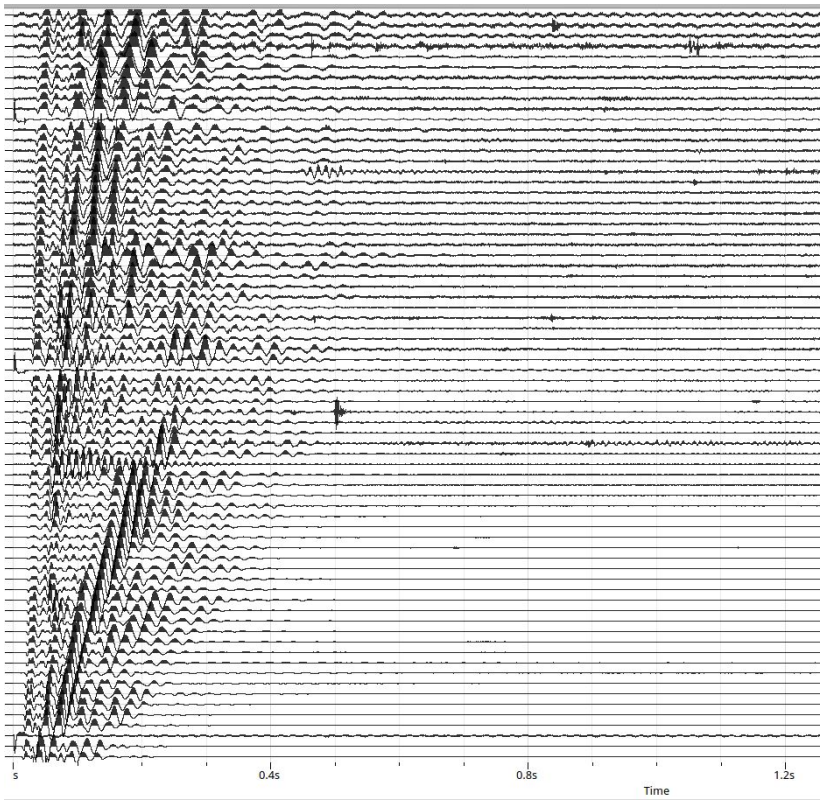

Figure 12: Example of a time-domain signal recorded by the 1D linear array of geophones. The shot was located at 5 m far from the last geophone (channel number #72).

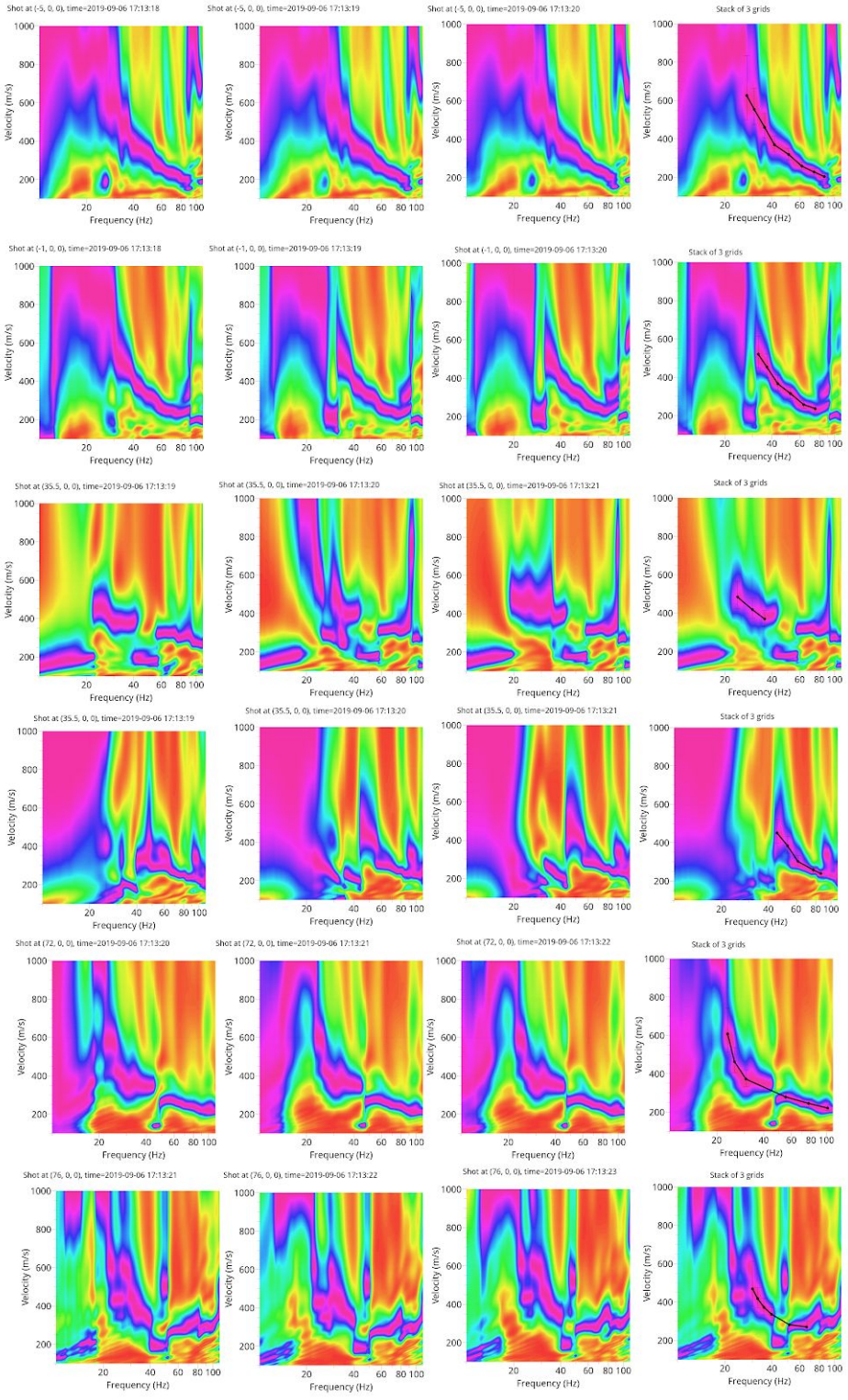

Figure 13: f-k results from the 1D linear active array. All the shots are shown; graphs in the same horizontal position refer to the same offset and the last column is their stack. The offset is varying from the top (-5 m from geophone #1) to the bottom panel (+5 m from geophone #72). For the middle shots (offset 35.5 m), 6 graphs are shown because the array line is shared in two (reverse from geophones #1 and #36 and forward from geophones #37 and #72).

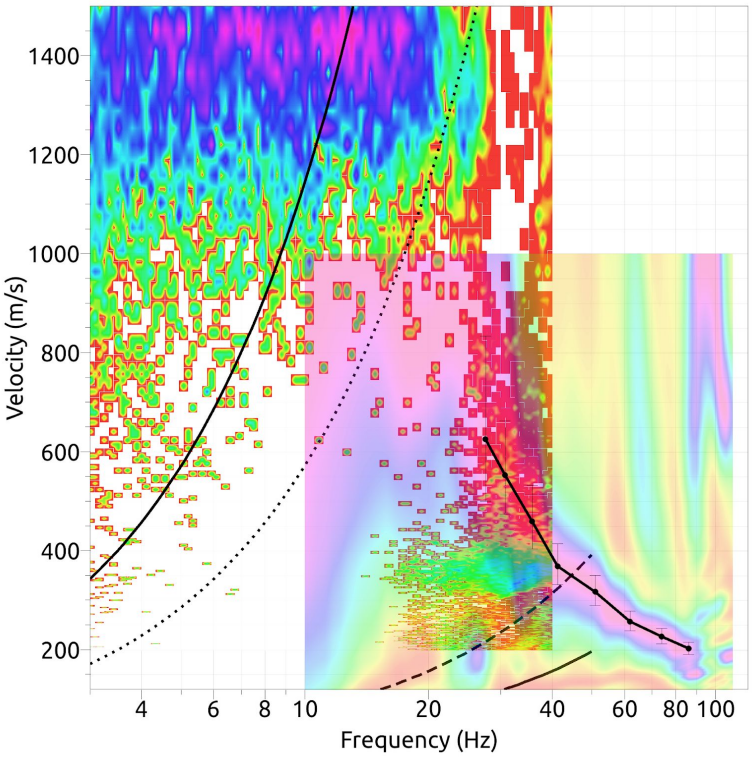

Figure 14: f-k comparison between the results obtained through the 2D passive array and 1D active array (in the last case the stack at offset -5 m was plotted).

3. SEISMIC VELOCITY MODEL

From Fig. 13, we selected the dispersion curves at offset -5 and -1 m that look more continuous in the frequency band of analysis. We computed the average curve resulting from these two offsets (Fig. 15). The average curve was resampled with 30 samples and was our target in the surface-wave inversion aimed at recovering the shear-wave (Vs) velocity model.

To proceed with the inversion step, we assume that the dispersion curve derived from the vertical geophones is associated to the fundamental mode of Rayleigh waves.

The resulting models obtained through the inversion of the dispersion curve are shown in Fig. 16. We tested several model parameterization composed of one or two main layers over halfspace, where in the first layer a shear-wave velocity increasing with depth was also allowed (following a linear-law or a power-law).

The Vs models (Fig.s 16 and 17) show velocity values increasing from 200 m/s up to 1000 m/s in the uppermost layer (about 10 m thick). The halfspace is therefore found by the inversion at 11 m deep,. The compressional velocity (Vp) models are also characterized by high velocity starting from few m deep. The best Vp and Vs models (i.e. lowest misfit) resulting from the inversion are proposed in Fig. 17 and Table 1.

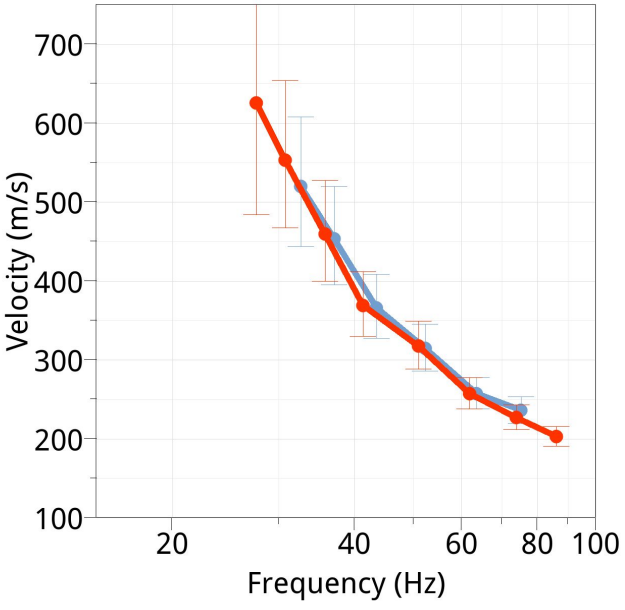

Figure 15: Dispersion curves obtained from the offset -1 and -5 m (blue and red curves, respectively). The average of the two curves provided the target dispersion curve used in the inversion step.

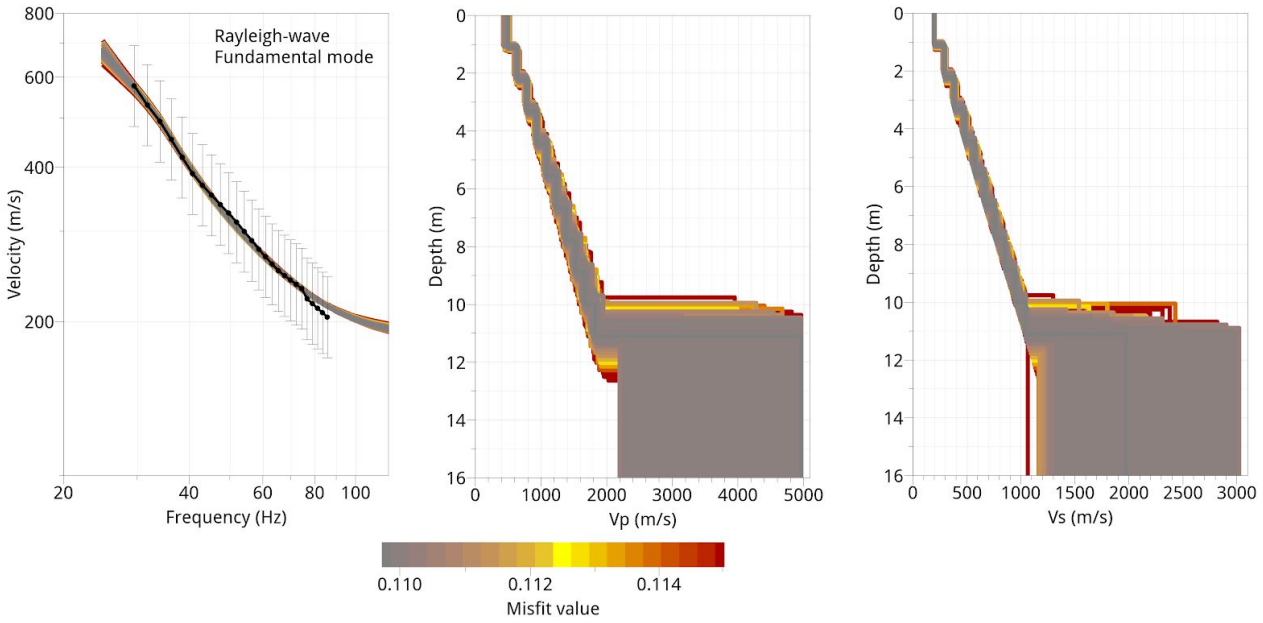

Figure 16: Models after the inversion of the dispersion curve (the field dispersion is shown as black curve). The best Vs model is presented in Fig. 17.

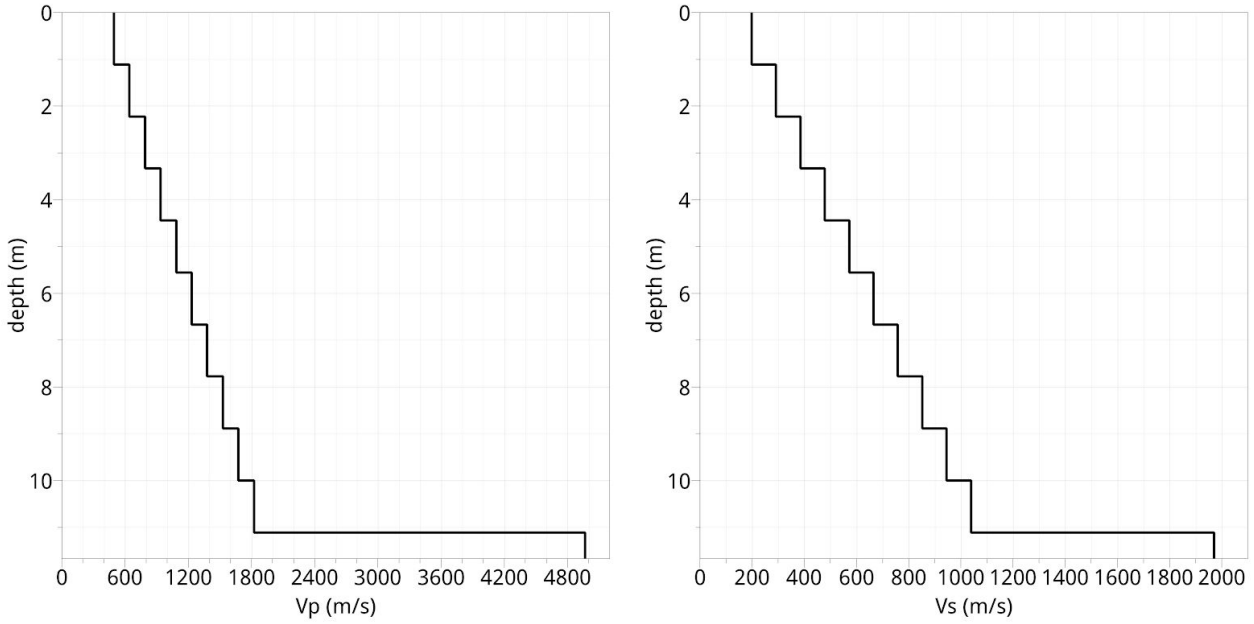

Figure 17: Best Vp and Vs model.

From (m)	To (m)	Thickness (m)	Vs (m/s)	Vp(m/s)
0	1.1	1.1	197	490
1.1	2.2	1.1	290	638
2.2	3.3	1.1	384	786
3.3	4.4	1.1	477	934
4.4	5.6	1.2	570	1082
5.6	6.7	1.1	664	1229
6.7	7.8	1.1	757	1377
7.8	8.9	1.1	851	1525
8.9	10	1.1	944	1673
10	11.1	1.1	1038	1821
11.1	1011.1	1000	1969	4963

Table 1: Best-fit model.

4. CONCLUSIONS

Surface-wave analysis at IV.TERO station indicates a stiff site. The HV noise spectral ratios are almost flat, although we found for some noise measurements a low-frequency peak (at 0.4 Hz) that we believe not reliable (see discussion in paragraph 2.1). A weak HV peak (amplitude level of about 2) seems present at 1.3 Hz.

The 2D passive circular array of geophones does not provide us a dispersion curve, in according with the difficulty to recognize dispersion features with passive technique in stiff site. In contrast, the 1D active linear array of geophones provides a dispersion curve up to 30 Hz (with apparent velocities of about 600 m). The inversion of the dispersion curve shows velocity models with a Vs increasing from 197 to 1038 m/s in the uppermost 11 m (Fig.s 16, 17 and Table 1).

The V_{S30} retrieved from the best inverted model is 981 m/s (Table 2), therefore IV.TERO is classified as soil class A also taking into account the geological information (see the Geological Report associated to the same station, http://hdl.handle.net/2122/12959). In the specific, both NTC08 or EC8 indicate a maximum thickness of an uppermost altered layer of few meters (3 or 5 meters, respectively), and this altered layer in our best model is slightly thicker. Following the definition of $V_{S,eq}$ within NTC18 and because the value of 800 m/s is reached at a depth of 7.8 m, the $V_{S,eq}$ is equal to 395 m/s and the soil class changes to B.

V_{S30} (NTC08 or EC8)	**Soil Class**
981 m/s	A

$V_{S,eq}$ (NTC18)	**Soil Class**
395 m/s	B

Table 2: Soil class following NTC08 and NTC18.

5. REFERENCES

EC8. CEN (2004), Eurocode (EC) 8: Design of structures for earthquake resistance – Part 1 General rules, seismic actions and rules for buildings (EN 1998-1), Brussels

Di Naccio, D., Famiani D. (2019). Geological Report at the seismic station IV.TER0- Teramo (TE) (December 2019). http://hdl.handle.net/2122/12959

Luzi L, Puglia R, Russo E & ORFEUS WG5 (2016). *Engineering Strong Motion Database, version 1.0*. Istituto Nazionale di Geofisica e Vulcanologia, Observatories & Research Facilities for European Seismology. doi: 10.13127/ESM"

NTC08, 2008. Ministero delle infrastrutture e dei Trasporti (2008). Norme Tecniche per le Costruzioni (NTC08). Decreto Ministero Infrastrutture. GU Serie Generale n. 29 del 04-02-2008 - Suppl. Ordinario n. 30

NTC18, 2018. Ministero delle infrastrutture e dei Trasporti (2018). Norme Tecniche per le Costruzioni (NTC18). Decreto Ministero Infrastrutture. GU Serie Generale n. 42 del 20-02-2018 – Suppl. Ordinario n. 8

Disclaimer and limits of use of information

The INGV, in accordance with the Article 2 of Decree Law 381/1999, carries out seismic and volcanic monitoring of the Italian national territory, providing for the organization of integrated national seismic network and the coordination of local and regional seismic networks as described in the agreement with the Department of Civil Protection.

INGV contributes, within the limits of its skills, to the evaluation of seismic and volcanic hazard in the Country, according to the mode agreed in the ten-year program between INGV and DPC February 2, 2012 (Prot. INGV 2052 of 27/2/2012), and to the activities planned as part of the National Civil Protection System.

In particular, this document1 has informative purposes concerning the observations and the data collected from the monitoring and observational networks managed by INGV.

INGV provides scientific information using the best scientific knowledge available at the time of the drafting of the documents produced; however, due to the complexity of natural phenomena in question, nothing can be blamed to INGV about the possible incompleteness and uncertainty of the reported data.

INGV is not responsible for any use, even partial, of the contents of this document by third parties and any damage caused to third parties resulting from its use.

The data contained in this document is the property of the INGV.

---

1 This document is level 3 as defined in the "Principi della politica dei dati dell'INGV (D.P. n. 200 del 26.04.2016)"

Esclusione di responsabilità ``e limiti di uso delle informazioni

L'INGV, in ottemperanza a quanto disposto dall'Art.2 del D.L. 381/1999, svolge funzioni di sorveglianza sismica e vulcanica del territorio nazionale, provvedendo all'organizzazione della rete sismica nazionale integrata e al coordinamento delle reti sismiche regionali e locali in regime di convenzione con il Dipartimento della Protezione Civile.

L'INGV concorre, nei limiti delle proprie competenze inerenti la valutazione della Pericolosità sismica e vulcanica nel territorio nazionale e secondo le modalitaà concordate dall'Accordo di programma decennale stipulato tra lo stesso INGV e il DPC in data 2 febbraio 2012 (Prot. INGV 2052 del 27/2/2012), alle attività previste nell'ambito del Sistema Nazionale di Protezione Civile.

In particolare, questo documento1 ha finalità informative circa le osservazioni e i dati acquisiti dalle Reti di monitoraggio e osservative gestite dall'INGV.

L'INGV fornisce informazioni scientifiche utilizzando le migliori conoscenze scientifiche disponibili al momento della stesura dei documenti prodotti; tuttavia, in conseguenza della complessità dei fenomeni naturali in oggetto, nulla può essere imputato all'INGV circa l'eventuale incompletezza ed incertezza dei dati riportati.

L'INGV non è responsabile dell'utilizzo, anche parziale, dei contenuti di questo documento da parte di terzi e di eventuali danni arrecati a terzi derivanti dal suo utilizzo.

La proprietà dei dati contenuti in questo documento è dell'INGV.

---

1 Questo documento rientra nella categoria di livello 3 come definita nei "Principi della politica dei dati dell'INGV (D.P. n. 200 del 26.04.2016)".